Earthquake Engineering, Tenth World Conference © 1992 Balkema, Rotterdam. ISBN 90 5410 060 5

Lateral pressure requirement for compressive concrete

S. Hatanaka
Mie University, Tsu, Japan
Y. Tanigawa
Nagoya University, Japan

ABSTRACT: A series of triaxial compression tests of normal and high strength concrete have been carried out by using a steel ring confinement. Based on the test results, the earlier proposed stress-strain model for concrete under triaxial compression has been extended to be applicable to the concrete of higher compressive strength up to 1000kgf/cm² and under higher confining pressure up to 50 kgf/cm². Further, quantitative discussion has been carried out on how much lateral confining pressure is required to keep concrete ductile, based on the proposed stress-strain model.

1 INTRODUCTION

The authors (1984,1985,1987,1990) have reported a series of study on the plastic deformation behavior of axially loaded concrete with low lateral confining pressure, aiming at a systematic evaluation of compressive toughness improvement due to various types of lateral confinements, based on the triaxial behavior of concrete.

As is already well known, compressive failure of concrete becomes more brittle as the compressive strength increases. Therefore, in order to keep concrete ductile, larger confining pressure is required for the higher strength concrete.

There are two main purposes in the present study. One is to extend the applicability of earlier proposed stress-strain model for concrete under triaxial compression to the higher strength and higher confining pressure level, based on the triaxial test result of high strength concrete. The other is to examine quantitatively how much lateral confining pressure is required to keep concrete ductile for the various strength of concrete.

2 EXPERIMENTAL PROCEDURES

Outline of experiment is shown in Table 1. Testing variables include the water-cement (W/C) ratio and the magnitude of lateral pressure (σ_L). All the specimens were cylinders of 10cm in diameter and 10cm in height. For the fabrication of specimen, ordinary Portland cement, river sand (less than 5mm), crushed stone (5-15mm), superplasticizer, and steel ring (inner diameter: 10cm, thickness: 3.2mm, width: 2.6, 5.2, and 10.4mm) were used. Slump was designed to be 15cm and compressive strengths to be 300, 500, 700, and 1000 kgf/cm².

Calculated lateral confining pressure by the steel ring (hereinafter, hoop) at the yielding is shown in Table 2. Specimens of W/C=0.55 were capped at the age of 1 day and demolded at the age of 2 days, while specimens of

Table 1 Outline of experiment

section (cm)	H/D	W/C	σ_C' (kgf/cm²)	σ_L (kgf/cm²)
φ10	1	0.55	300	0
		0.42	500	12.5
		0.32	700	25.0
		0.22	1000*	50.0

*only for σ_L= 50 kgf/cm², H/D : Hight/diameter of specimen, W/C : Water-cement ratio, σ_C' :Designed compressive strength, σ_L : Designed lateral pressure

Table 2 Calculated lateral confining pressure at yielding of hoops

f_y (kgf/cm²)	S (mm)	t (mm)	d (mm)	$_H\sigma_{LY}$ (kgf/cm²)
1950	25	3.1	2.6	12.6
			5.2	25.1
			10.4	50.3

f_y : Yield strength of steel, S : Pitch, t : Thickness of hoop, d : Width, $_H\sigma_{LY}$: Calculated lateral pressure when steel hoops yield

$$_H\sigma_{LY} = \frac{2 \cdot t \cdot d}{S \cdot D} \times f_y$$

W/C=0.42, 0.32, and 0.22 were capped at the age of 6 hours and demolded at the age of 1 day. All the specimens were cured in a moist room (27±1℃, relative humidity: 88±2%) and tested at the age of about 50 days. The number of specimens for each combination of factors was 2.

Specimens were loaded in an actuator type testing machine (capacity: 200 tf) under the constant strain rate of about 1×10^{-3}/min. up to the specified longitudinal strain ($\varepsilon_1=20\times10^{-3}$). Friction at the specimen-loading platen interfaces was reduced by placing friction reducing pads which consists of two polypropylene sheets with silicon grease between them.

The longitudinal strain in the stress ascending range was measured by a couple of deformation transducers attached to a specimen by means of steel frames, while in the stress descending range, the steel frames were taken away and strain was measured by another couple of deformation transducers set between loading plates. The strain (ε_L) of hoops were also measured by couples of wire strain gauges (W.S.G.) attached to specified hoops.

3 TEST RESULTS AND DISCUSSION

3.1 Strain of hoops and lateral pressure

Figures 1(a) through (d) show the examples of variation of hoop strain and Figs.2(a) through (d) show the lateral pressure ($_H\sigma_L$) curves calculated from the data as in Fig.1.

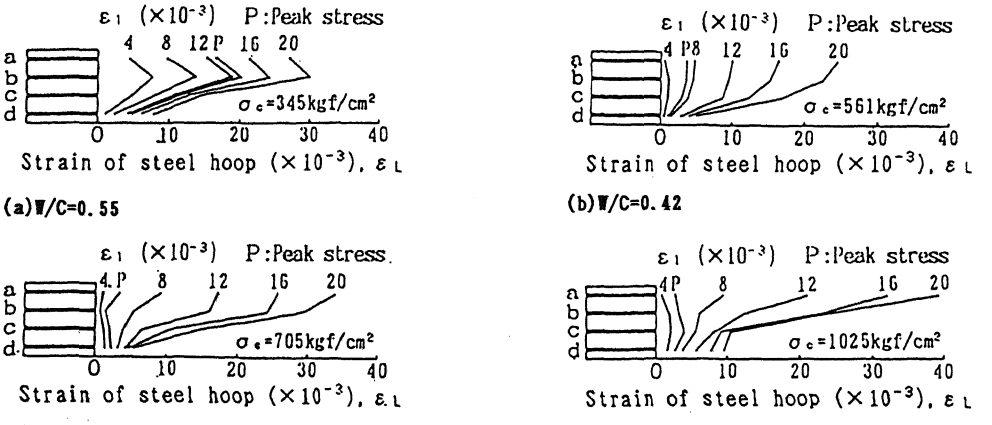

Fig.1 Variation of strain of hoops ($_H\sigma_{LY}$=50.3kgf/cm²)

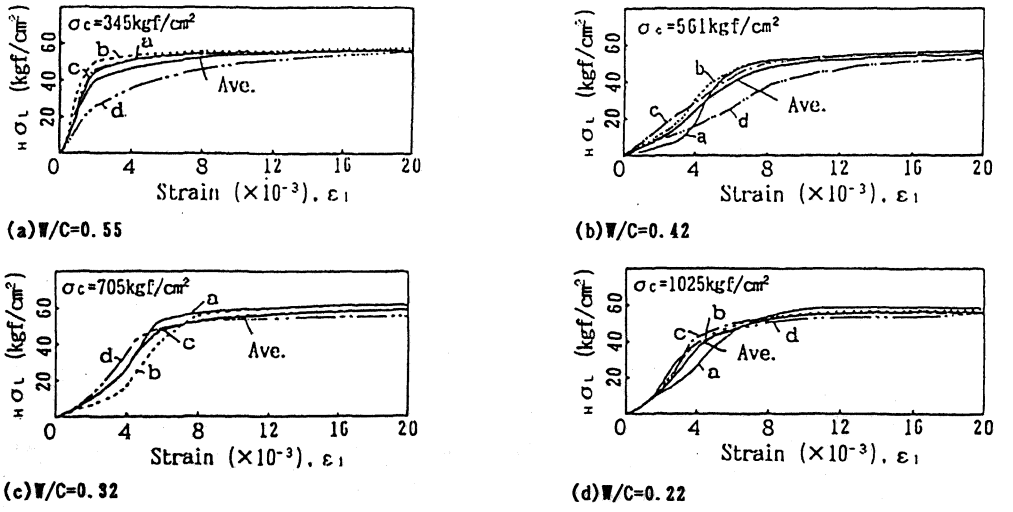

Fig. 2 Variation of lateral pressure ($_H\sigma_L$) calculated from the strain of hoops ($_H\sigma_{LY}$=50.3kgf/cm²)

According to these figures, lateral pressure is applied almost uniformly to specimens regardless of concrete strength, although the strain of hoops tends to be large in the upper part (upper side in casting) of specimen. Therefore, the present experiment can be considered to be a triaxial compressive test with passive type lateral pressure.

3.2 Modification of stress-strain curve

Measured longitudinal stress (σ_1)-longitudinal strain (ε_1) curves were modified, so that lateral pressure after the peak stress keeps constant value. Figure 3 shows examples of comparison between measured and modified curves, where the value of measured lateral pressure ($_H\sigma_L$) is the average of the calculated lateral pressure in Fig.2. Figure 4 illustrates the method of modification, which was done on the assumption that the increment ($\sigma_1^*-\sigma_0$) of the load-carrying capacity of concrete specimen due to lateral pressure (σ_L^*) is proportional to the magnitude of lateral pressure (σ_L^*) at the same strain level.

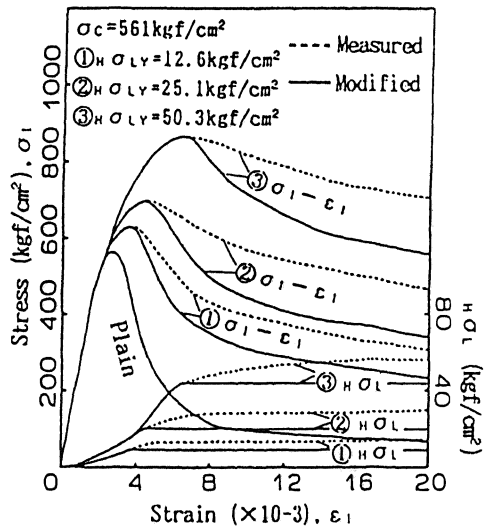

Fig.3 Comparison between measured and modified $\sigma_1-\varepsilon_1$ curves (W/C=0.42)

4 STRESS-STRAIN MODEL

4.1 Extension of applicability of model

The authors (1987,1990) have already proposed a longitudinal stress-strain model for concrete under triaxial compression, incorporating the failure criterion proposed by N.S.Ottosen (1977). The range of its applicability, however, is up to about compressive strength σ_c=700 kgf/cm² and σ_L=15 kgf/cm². The proposed model is being modified based on the present test data.

(1) Stress and strain at peak point

Figure 5 shows the ratio of lateral pressures ($\omega=\sigma_A/{}_H\sigma_{LP}$); where, σ_A is the lateral pressure (active pressure σ_A) calculated by putting the experimental maximum stress into the failure criterion in Table 3, and $_H\sigma_{LP}$ is the lateral pressure calculated directly from the strain of hoops. As seen in the figure, most of the values of ω are smaller than 1.0. The main reasons are considered to be:

i) The loading path of the lateral pressure is active in general triaxial compression tests, while it is passive in the present experiment.

ii) The distribution of the lateral pressure is uniform in general triaxial compression tests, while it is not necessarily uniform in the present experiment (see Fig.2).

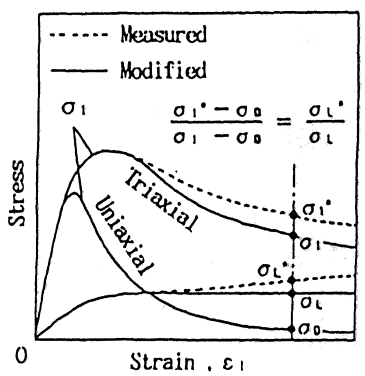

Fig.4 Modification method of $\sigma_1-\varepsilon_1$ curves

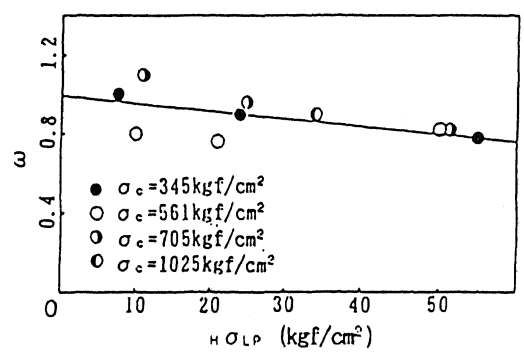

Fig.5 $\omega-{}_H\sigma_{LP}$ relation

The value of ω tends to decrease with the increase in lateral pressure ($_H\sigma_{LP}$), and is expressed in the following equation.

$$\omega = 1 - 0.004_H\sigma_{LP} \quad (1)$$

Therefore, the lateral stress (σ_A) which is to be put in a failure criterion is

$$\sigma_A = \omega \cdot {}_H\sigma_{LP} \quad (2)$$

On the other hand, experimental values of the strain (ε_{1P} for passive lateral pressure) at the peak stress are almost the same as the calculated ones (ε_{1A} for active lateral pressure) from the earlier proposed equation (see Table 3).

(2) Stress-strain relation

Figures 6(a) through (c) show the comparison between predicated and modified experimental σ_1-ε_1 curves. Here, peak stress is calculated by incorporating Eq.(2) in the failure criterion in Table 3, and the reduction rate (ω) of the effective lateral pressure is assumed to be constant at every strain level. It is shown that σ_1-ε_1 curves of W/C=0.55 are well predicted by using the earlier proposed model (1987); while in W/C=0.42 and 0.32, calculated curves differ gradually from the experimental ones in the lateral pressure level of over 20 kgf/cm². The earlier proposed model is modified to be applicable to the concrete of higher compressive strength and under higher confining pressure. The parameters (p, q, r) which determine the descending portions are slightly changed. The modified σ_1-ε_1 model is shown in Table 3. Calculated curves by using the modified model is also shown in Figs.6(a) through (c). Fairly good agreement is observed.

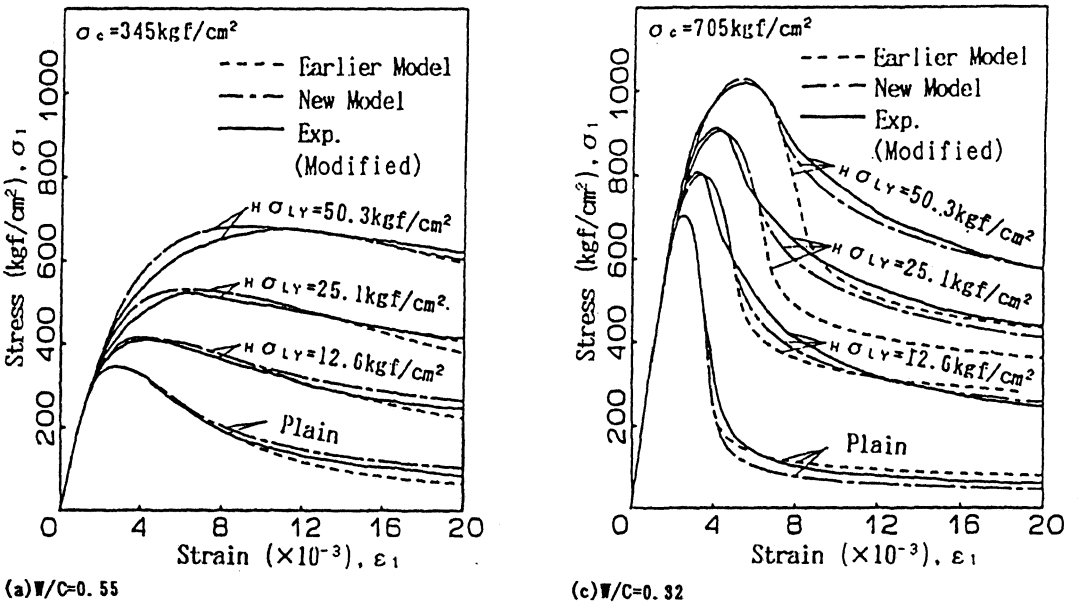

Fig.6 Comparison between predicted and modified experimental $\sigma_1 - \varepsilon_1$ curves

Table 3 Stress(σ_1)−strain(ε_1) model

(a) Failure Criterion

Stress	Strain
In Ottosen's eq., $A=1.2566$, $B=4.0301$ $k_1=14.6334$, $k_2=0.9870$	$\dfrac{\varepsilon_{1f}}{\varepsilon_c}=a\left(I_{1f}/\sigma_c-1\right)+1$

I_{1f}:First stress invariant at failure ($I_{1f}=\sigma_{1f}+\sigma_2+\sigma_3$), σ_{1f}, ε_{1f}: Stress and strain in the direction of maximum principal compressive stress, σ_c, ε_c:Stress and strain at uniaxial failure, a :Empirical constant ($a=2.0$)

(b) Relative Stress - Relative Strain Relation

Ascending Portion	Descending Portion
$\dfrac{\sigma_1}{\sigma_{1f}}=\dfrac{N_a\cdot E}{N_a-1+E^{N_a}}$	$\dfrac{\sigma_1}{\sigma_{1f}}=\dfrac{1}{N_d}+\dfrac{(N_d-1)\cdot X}{N_d-1+X^{N_d}}$

$N_a=E_i/(E_i-\sigma_{1f}/\varepsilon_{1f})$, E_i:Initial Young's Modulus, measured value or $E_i=2.1\times10^5\sqrt{\sigma_c/200}$, $X=E_1^m$, $E_1=E$ $(E<a)$, $E_1=\ln\{b(E-a)+1\}/b+a$ $(E\geqq a)$, $E=\varepsilon_1/\varepsilon_{1f}$, $a=p/(\sigma_c/100)+1$, $b=q\times10^{-3}(\sigma_c/100)^r$, $N_d=\alpha N_{d0}$, N_{d0}:N_d of uniaxial comp., α, p, q, r :Empirical const. ($p=200/(\sigma_L+50)$, $q=5.5$, $r=3.8$, $\sigma_L=\sigma_2=\sigma_3$)

(c) Constants for Uniaxial Stress-Strain Relation (Comp.)

N_{d0}	m	α $(0\leqq\alpha\leqq1)$
$(\sigma_c<360)$ $1+6(\sigma_c/100)^{0.6}$ $(\sigma_c\geqq360)$ $1+(\sigma_c/100)^{2.8}$	0.2	$(1.0\leqq S_f\leqq1.15)$ $\alpha=3-2S_f$ $(S_f\geqq1.15)$ $\alpha=0.7$

$S_f=\sigma_{1f}/\sigma_c$

4.2 Lateral pressure required for sufficient compressive ductility

Figure 7 shows the lateral pressure ($_R\sigma_L$) required to maintain the stress as large as uniaxial compressive strength even after the peak stress point (hereinafter, non-softening type). The magnitude of $_R\sigma_L$ increases with increasing strain after the peak stress point, and reaches almost constant value at the high strain level of $\varepsilon_1=20\times10^{-3}$.

Figure 8 shows the change in the values of $_R\sigma_L$ for various strength level of concrete. Here, the strain (ε_c) at the peak stress point is assumed to be constant as $\varepsilon_c=2.5\times10^{-3}$. It is shown that the value of $_R\sigma_L$ increases with the increase in the compressive strength of concrete, and that rapid increase in the lateral pressure is required just after the peak stress point ($\varepsilon_c=2.5\times10^{-3}$) for high strength concrete.

Figure 9 shows the approximate value of $_R\sigma_L$ for various strength level of concrete, where the value of $_R\sigma_L$ for $\varepsilon_1=(10\sim20)\times10^{-3}$ is plotted. According to the figure, the approximate value of $_R\sigma_L$ is $\sigma_c/20$. Note

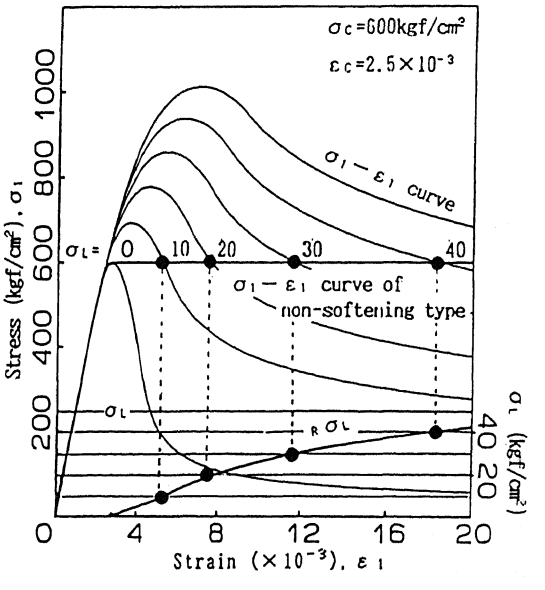

Fig. 7 Change in lateral pressure (σ_L) required for non-softening type $\sigma_1-\varepsilon_1$ curve

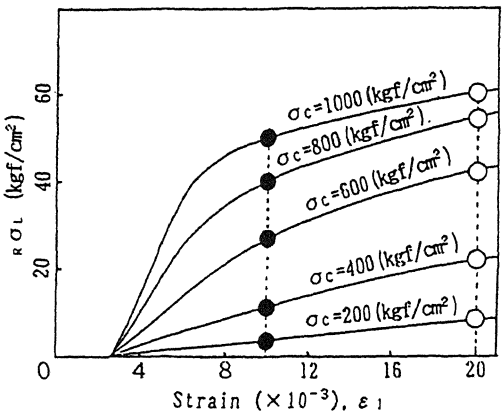

Fig.8 Change in required lateral pressure ($_R\sigma_L$)

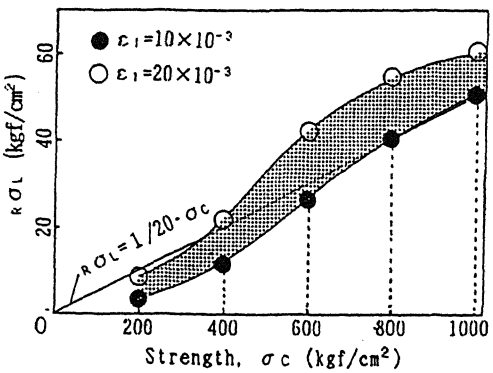

Fig.9 Required lateral pressure ($_R\sigma_L$) for various strength of concrete

that the reduction of the effectiveness of lateral pressure due to the passive path of loading is not taken into consideration in the present discussion. Much more lateral pressure is considered to be required for the assurance of the sufficient ductility of actual confined concrete, in which lateral pressure is to be exerted passively on concrete.

5 CONCLUSIONS

1) The earlier proposed stress-strain model for concrete under triaxial compression is extended to be applicable to the concrete of higher compressive strength up to 1000 kgf/cm² and under higher confining pressure up to 50 kgf/cm².

2) In order to keep concrete non-softening type or to maintain the stress as large as uniaxial compressive strength σ_c, at least the following magnitude of lateral pressure ($_R\sigma_L$) is required: $_R\sigma_L \geq \sigma_c/20$.

3) By using the present stress-strain model, systematic discussion based on the confining pressure can be carried out on the effectiveness of various types of lateral confinements, which will be the next target of the future study.

ACKNOWLEDGMENT

The authors are very grateful to Messrs. H.Hattori and Y.Kondo for their cooperation.

REFERENCES

Hatanaka,S., Kosaka,Y. and Tanigawa,Y. 1987. Plastic Deformational Behavior of Axially Loaded Concrete under Low Lateral Pressure. J. Struct. and Const. Eng. (Trans. of Architectural Institute of Japan). 377: 27-40.

Hatanaka,S., Hattori,H., Yoshida,N. and Tanigawa,Y. 1990. Compressive Deformation Capacity of High Strength Concrete under Low Lateral Confining Pressure. Trans. Japan Conc. Inst. 12: 151-158.

Kosaka,Y., Tanigawa,Y., and Hatanaka,S. 1984. Inelastic Deformational Behavior of Axially Loaded Concrete under Low Lateral Confining Stresses. Trans. Japan Conc. Inst. 6: 257-260.

Kosaka,Y., Tanigawa,Y., and Hatanaka,S. 1985. Lateral Confining Stresses Due to Steel Fibres in Concrete under Lateral Confinement, Int'l J. Cem. Compo. 7-2: 81-92.

Ottosen,N.S. 1977. A Failure Criterion for Concrete, J. EM Div. ASCE. 103-EM4: 527-535.